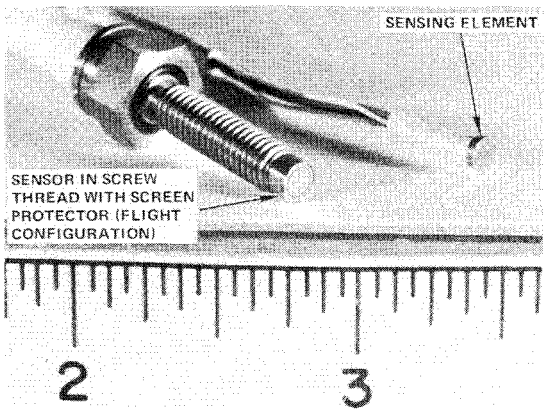


Fig. 2 Solid state pressure sensor for flight experiment.

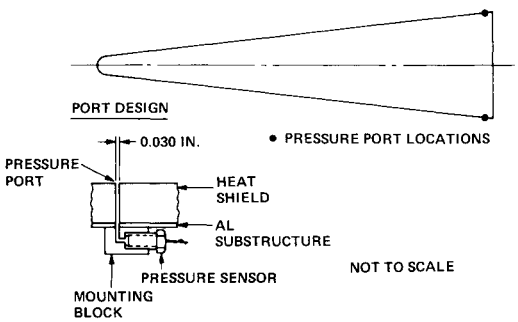


Fig. 3 Flight 2 re-entry vehicle configuration.

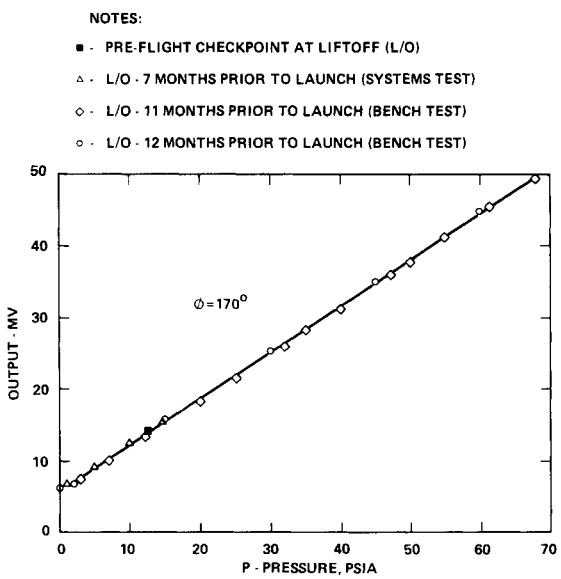


Fig. 4 Pressure sensor calibration curve.

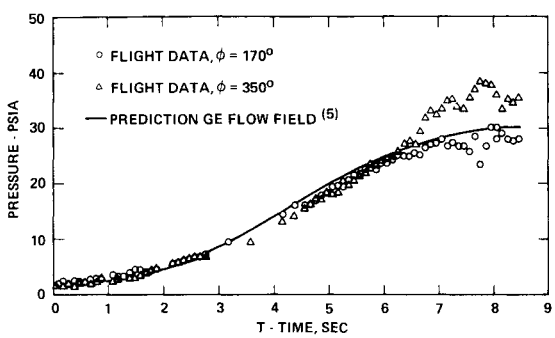


Fig. 5 Forebody flight test pressure data in laminar and turbulent flow: flight 2.

(Fig. 3). The two diametrically opposed pressure ports were located 98% of the vehicle length and utilized a 0.030-in. diam hole with a right-angle configuration. The small port diameter was chosen to minimize pressure port erosion effects in turbulent flow.[4]

The pressure sensors were calibrated several times prior to lift-off ranging from 7 to 12 months and a preflight check point a few minutes prior lift-off was obtained. A typical calibration curve for one sensor is presented in Fig. 4. Agreement among data points is generally good. The preflight lift-off checkpoint shows that the sensor was stable since the calibration curve had not shifted prior to the flight.

The reduced flight data for the diametrically opposed ports are shown in Fig. 5. The flight data are in good agreement with the GE flowfield predictions[5] for both laminar and turbulent flow. For times greater than 7 sec the pressure data show a pressure differential of $\approx$ 10 psia which is due to R/V angle of attack.

## Conclusions

The flight test experiment has met its objective and has demonstrated that the miniaturized solid state pressure sensor can measure steady-state pressures in an R/V flight test application. Forebody pressure data were obtained in laminar and turbulent flow on a slightly blunted slender cone using the solid-state pressure sensor. The flight data were found to be in basic agreement with flowfield predictions.

## References

[1] Cassanto, J. M., Rogers, D. A., Droms, C. R., and Robinson, A. G., "Use of a Minature Solid State Pressure Transducer for R/V Flight Test Application," *Proceedings of the 20th International Instrumentation Symposium,* Instrument Society of America, ISA Paper 74210, 1974; also GE-RESD TIS 74SD210, Dec., 1974.

[2] Cassanto, J. M. and Rogers, D. A., "An Experiment to Determine Nose Tip Transition with Fluctuating Pressure Measurements (Ground Test Data)," AIAA Paper 74-625, Bethesda, Md., 1974.

[3] "Notes on Applications of Integrated Sensor (IS) Pressure Transducer," Application Note KPS AN 11, Kulite Semi Conductor Products, Inc., Ridge Field, N.J.

[4] Cassanto, J. M., "An Assessment of Pressure Port Erosion Effects," AIAA Paper 75-150, Pasadena Calif., Jan. 1975.

[5] Storer, E. M., "Summary of Flow Field Solution on Sphere Cones at Several Mach Numbers and Altitudes," ATDM 67-12, March 1967, General Electric Co., Philadelphia, Pa.

# Energetic Solar Proton vs Terrestrially Trapped Proton Fluxes

J. H. King* and E. G. Stassinopoulos*
*NASA Goddard Space Flight Center, Greenbelt, Md.*

## Introduction

THIS Note is intended to demonstrate the relative importance of solar and trapped proton fluxes in the consideration of shielding requirements for 1977-1983 geocentric space missions. Using the latest solar proton[1] and trapped proton[2,3] models, fluences of these particles encountered by spacecraft in circular orbits have been computed as functions of orbital altitude and inclination, mission duration, threshold energy (between 10 and 100 MeV), and, for solar

Received August 27, 1974; revision received November 4, 1974.
Index category: Radiation Protection Systems.

*Space Data Acquisition Scientist, National Space Science Data Center.

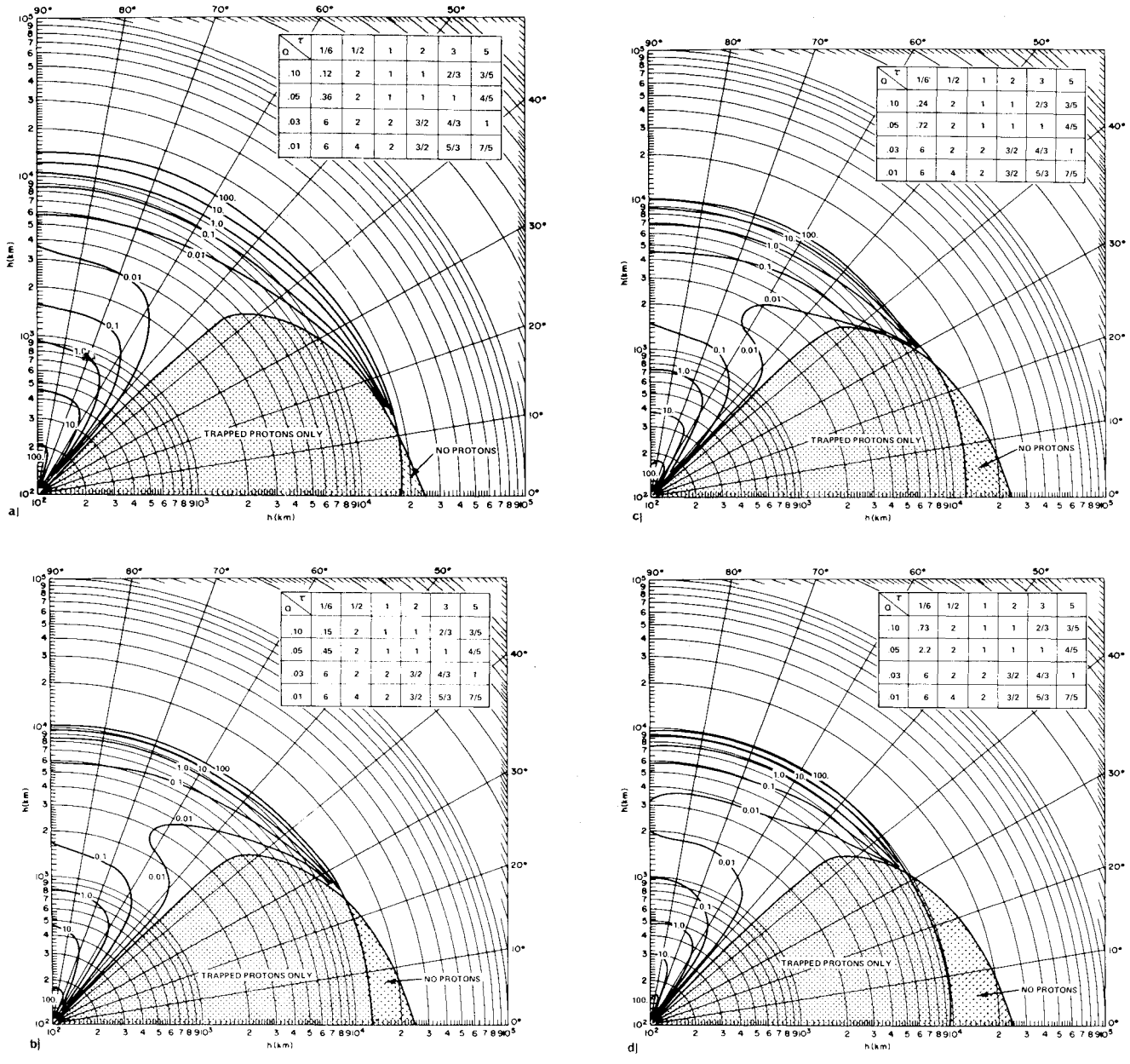


**Fig. 1 Constant value contours for ratios of solar-to-trapped proton fluences as a function of orbit altitude and inclination for 1 year missions and for 10% risk factor. Inset matrix gives multiplication factors for other mission durations ($\tau$, in years) and risk factors ($Q$): a) $E_p > 10$ Mev; b) $E_p > 30$ Mev; c) $E_p > 50$ MeV; d) $E_p > 100$ MeV.**

proton fluxes, risk factor.† Ratios of solar-to-trapped proton fluences were then taken. These ratios give the relative importance of the two proton populations and indicate to the mission planner whether he must consider both or only one of these populations. To determine the absolute fluence level of either population, the mission planner must refer to one of the sources already cited.

## Calculations

It is desired to specify the ratio $R$:

$$R(h,i;E;\tau,Q) = \frac{S(h,i;E;\tau,Q)}{T(h,i;E;\tau)} \quad (1)$$

Here $S$ and $T$ are fluences associated with solar and trapped protons, respectively. The independent variables are: $h$ and $i$, the altitude and inclination of the circular orbit; $E$, the proton energy threshold; $\tau$, the mission duration; and $Q$, the risk factor. Note that, owing to the statistical and deterministic natures of solar and trapped fluences respectively, $S$ is a design fluence which may or may not occur, while $T$ is the trapped proton fluence which the spacecraft is actually expected to encounter.

From Ref. 1, we have

$$S(h,i;E;\tau,Q) = S_1(h,i) \times [S_2(E)S_3(\tau,Q) + S_4(E;\tau,Q)] \quad (2)$$

Here $S_1(h,i)$ represents orbit-integrated effect of geomagnetic shielding (energy independent owing to assumed $L=5$ cutoff for all protons[1,4]), $S_2(E)$ gives the integral flux and spectrum of each anomalously large event (assumed to replicate the Aug. 1972 event), while $S_3(\tau,Q)$ gives the number of such events expected, and $S_4(E;\tau,Q)$ gives the fluence contributed by ordinary events. For values of $\tau$ and $Q$ such that $S_3 > 0$, we may take $S_4 = 0$. The solar proton model used is for the solar active period 1977-1983. As such, this analysis should not be applied during solar quiet times.

†Risk factor: a parameter expressing the chance a mission planner is willing to take that the actually encountered fluxes will exceed the predicted levels.

For time scales long compared to one orbital period, the trapped proton fluences are obtained from

$$T(h,i;E;\tau)=T_1(h,i;E)\times\tau \tag{3}$$

where $T_1$ is an annual trapped proton fluence and $\tau$ is the mission duration in units of years.

With Eqs. (2) and (3), the ratio $R$ may be rewritten as

$$R(h,i;E;\tau,Q)=R_1(h,i;E)R_2(E;\tau,Q) \tag{4}$$

where $R_1=S_1S_2/T_1$ and $R_2=\tau^{-1}\times(S_3+S_4/S_2)$. The $R_1$ functions have the significance of being the solar-to-trapped proton fluence ratios for 1-year missions for which exactly one anomalously large event must be anticipated. $R_1$ functions are plotted in Figs. 1a-1d in terms of iso-ratio contours in $h$-$i$ space for a series of energy thresholds. The $R_2$ functions are $R_1$ modifiers, adjusting the ratios to reflect the $Q$, $\tau$ dependent variation in mission duration and in the number of anomalously large events to be expected. Values of $R_2$ are inserted in matrix form into Figs. 1a-1d for mission duration between 2 months and 5 years and for risk factors between 0.01 and 0.1 (1 and 10%). Note that $R_2$ values are independent of energy for all $Q$, $\tau$ matrix elements except for the 5 and 10% risk factors of the 2-month missions, for which no anomalously large event is predicted. For all other elements, $S_3>0$ and $S_4/S_2$ becomes insignificant.

## Discussion

The accuracy of the figures reflects the accuracy of the models used. As discussed in Ref. 4, the common geomagnetic cutoff assumption of the solar proton model used is reasonable for protons of less than 100 MeV, but becomes progressively less accurate as energies increase above 100 MeV. Thus, in Fig. 1d, the $R_1$ function may be underestimated by a factor of up to two. Likewise, there is a typical uncertainty by a factor of about two in the trapped proton model used.

Many features are immediately visible in the figures. First of all, the solar-to-trapped ratio is zero for orbits in the shaded areas where, by virtue of geomagnetic shielding, no solar particle reaches a spacecraft anywhere along its orbit. In the cross hatched region (high altitude, low inclination) the ratio is meaningless because neither solar nor trapped protons reach the spacecraft.

At a fixed altitude (below a few hundred km or so) the dominant fluence source shifts rapidly from trapped to solar protons as orbit inclination is increased through the 50° to 60° range. Thus, for low-altitude, polar-orbiting spacecraft, solar protons are very important relative to trapped protons. As the altitude of a polar orbit mission is increased, the solar-to-trapped ratio declines and then increases again. This is mainly due to the low latitude portion of the orbit moving out to, and then beyond, the regions of maximum trapped particle fluxes. The energy dependence of $R_1$, apparent from a sequential examination of Figs. 1a-1d, results from the variability of the trapped proton spectrum at differing spatial points and the dissimilarity of the trapped and solar spectra.

By examination of the inset matrices in Figs. 1a-1d, it is apparent that for a fixed risk factor, solar particles tend to become relatively less important than trapped particles as mission duration increases. At fixed mission duration, however, solar protons become relatively more important than trapped particles as the permissible risk factor is decreased. Note, however, that as long as at least one anomalously large event is anticipated, the variation in the solar-to-trapped ratio due to the mission duration and risk factor dependences is very small relative to the variation associated with the altitude and inclination dependences.

## Conclusions

The purpose of the analysis has been to permit the space mission planner to readily determine whether he must consider solar and trapped proton fluences, or only one or the other, in his shielding requirements. The analysis is not intended to provide actual fluence values, which are available in the references cited.

The mission planner must specify orbit altitude and inclination (circular orbits only), mission duration, and the percent risk he is willing to take that the actually encountered solar proton fluence will exceed his design fluence. Then from the appropriate figure for the energy threshold of interest, he multiplies the appropriate factor from the inset matrix by the appropriate plotted $R_1$ value in order to determine the ratio of solar-to-trapped proton fluences he must allow for in his mission planning. Typically, interpolation will be required.

It is clear that for low-altitude polar and very high-altitude missions (any inclination), solar protons dominate trapped protons. Conversely, for low-inclination, low- and medium-altitude missions and for high-inclination, medium-altitude missions, trapped protons dominate the solar protons.

Due to the uncertainties in the models, we would recommend that if the value of the $S/T$ ratio fell between 0.1 and 10, the mission planner ought to consider both trapped and solar proton fluences. Likewise, if the desired $h$, $i$ point is in a region of rapidly changing $S/T$ ratio, both trapped and solar fluxes should be considered.

## References

[1] King, J.H., "Solar Proton Fluences for 1977-1983 Space Missions," *Journal of Spacecraft and Rockets,* Vol. 11, June 1974, pp. 401-408.

[2] Lavine, J. P. and Vette, J. I., "Models of the Trapped Radiation Environment, Vol. V: Inner Belt Protons," SP-3024, 1969, NASA.

[3] Lavine, J. P and Vette, J. I., "Models of the Trapped Radiation Environment, Vol. Vi: High Energy Protons," SP-3024, 1970, NASA.

[4] Stassinopoulos, E. G., and King, J. H., "Empirical Solar Proton Model for Orbiting Spacecraft Application," *IEEE Transactions on Aerospace and Electronic Systems,* Vol. AES-10, July 1974, pp. 442-450.

# Errors in Aerodynamic Heat Transfer Measurements when Using Phase Change Coating Techniques

John A. Segletes*
*Teledyne Isotopes, Timonium, Md.*

## Nomenclature

| | | |
|---|---|---|
| $CF$ | = | correction factor |
| $h$ | = | heat transfer coefficient |
| $k$ | = | thermal conductivity |
| $T$ | = | temperature |
| $x$ | = | distance from surface |
| $X, Y, \tau$ | = | see Eq. 1 |
| $\alpha$ | = | thermal diffusivity |
| $\theta$ | = | time |

Received September 20, 1974; revision received Oct. 29, 1974. The work reported was supported under AEC Contract AT (49-15)-3069.

Index categories: Heat Conduction, Thermal Modeling and Experimental Thermal Simulation.

*Aerothermal Engineer, Safety and Reliability. Member AIAA.